JOURNAL OF GEOPHYSICAL RESEARCH, VOL. 106, NO. C2, PAGES 2313–2329, FEBRUARY 15, 2001

A global wave hindcast over the period 1958–1997: Validation and climate assessment

Andrew T. Cox
Oceanweather Inc., Cos Cob, Connecticut

Val R. Swail
Environment Canada, Toronto, Ontario, Canada

Abstract. This study describes the first 40 year global wave simulation derived from the National Centers for Environmental Prediction/National Center for Atmospheric Research Reanalysis (NRA) surface wind fields. The NRA 10 m wind fields were input into a deep water version of a proven spectral ocean wave model adapted onto a global grid of spacing 1.25° in latitude by 2.5° in longitude. In situ and satellite wind and wave data sets were used to evaluate the hindcast skill. The validation showed excellent agreement not only in terms of bias and scatter but over the entire frequency distribution out to 99th percentiles of both winds and waves. A global trend analysis showed statistically significant areas of both increasing and decreasing winds and waves. The increasing trend in the northeast Atlantic and decreasing trend in the central North Atlantic are particularly well defined and consistent with changes reported in previous studies, which were linked to changes in the North Atlantic Oscillation. The trend analysis highlighted the difficulty in separating creeping inhomogeneities in the NRA winds from real climate change, illustrating the need to use homogeneous in situ measured data to confirm trends derived from model output. The trends derived from the hindcast seem reasonable in the Northern Hemisphere and may provide a good upper bound to true trends in the wind and wave climate.

1. Introduction

The global ocean wave climate has long been of interest to the ocean engineering community because of the need for accurate extreme and operational wave data for applications such as vessel design, specification of peak loads of coastal and offshore structures, and planning of naval and marine operations. In recent years, there has been a major resurgence of interest in wave climate within the scientific community as a result of indications of worsening storm wave regimes in some areas [*Bacon and Carter*, 1991] and evidence that trends and variability in wave climate on a regional basis may be linked to more familiar modes of atmospheric climate trend and variability such as the North Atlantic Oscillation (NAO) [*Kushnir et al.*, 1997]. Even the response of the global wave climate to a possible global warming scenario has been studied using a general circulation model [*WASA Group*, 1998].

There have been several major attempts within the past 2 decades to develop long-term wave climatologies from continuous integrations of spectral ocean wave models applied to Northern Hemisphere basins. These include the U.S. Navy 20 year (1956–1975) Northern Hemisphere project using the Spectral Ocean Wave Model [*U.S. Naval Oceanography Command*, 1983], the U.S. Army 20 year (1956–1975) North Atlantic and North Pacific Oceans Wave Information Study (WIS) project using the WIS wave model [*Corson et al.*, 1981], a 35 year simulation of the North Atlantic Ocean carried out by the Norwegian Meteorological Institute using the Waves in the Norway Coast-Hindcasting (WINCH) model [*Eide et al.*, 1985], and a 40 year hindcast of the northeast Atlantic Ocean using the Wave Modelling Group (WAM) model [*Gunther et al.*, 1998]. Since the mid-1980s, several major numerical weather prediction (NWP) centers (U.S. Navy Fleet Numerical Meteorology and Oceanography Center (FNMOC), European Centre for Medium-Range Weather Forecasting (ECMWF), and U.S. National Centers for Environmental Prediction (NCEP)) have operated global spectral ocean wave models in real time and have accumulated the analysis products to form preliminary estimates of the global wave climate. Recently, the ECMWF wave model was applied to hindcast the 15 year period 1979–1993 [*Sterl et al.*, 1998].

The three most recent efforts noted above deserve further comment within the context of the present study. The study of *Kushnir et al.* [1997] involved a wave hindcast of the North Atlantic Ocean and covered a 10 year period. The wave model, essentially the same formulation used in the present study, was driven by ECMWF operational wind fields developed during the 1980s. Kushnir's analysis involved monthly means of hindcast significant wave heights (MMSWH) and was most significant because it applied canonical correlation analysis (CCA) to establish a link between the model MMSWH and the sea level pressure field. The extension back in time of the sea level pressure analysis using the CCA led to inference of patterns of trends in MMSWH over the period 1962–1986, resembling the dipole associated with the NAO. A direct verification of the inferred patterns of MMSWH trend, of course, could not be made except against measured wave data at two sites in the eastern North Atlantic (Seven Stones Light Vessel and Ocean

Paper number 2001JC000301.
0148-0227/01/2001JC000301$09.00

Station Lima) because the wave hindcast itself spanned only 10 years.

The hindcast carried out within the context of Waves and Storms in the North Atlantic (WASA) [*Gunther et al.*, 1998] used a third generation (3G) wave model and spanned the continuous 40 year period 1955–1994. That hindcast also considered only the North Atlantic Ocean and was driven by operational wind fields produced in real time by, and obtained by WASA from the historical archives of, the U.S. Navy. On the assumption that these wind fields (however, see below) are homogeneous, the hindcast was analyzed for trends in mean and extreme wave patterns. However, inhomogeneities and other problems with the hindcast in the area west of 20°W limited the reliability of the analysis to the extreme eastern North Atlantic, where it was concluded that the wave climate has undergone significant secular change consistent with the above noted trend.

One disturbing property of the earlier hindcast studies and of the real-time NWP operations is that changes over time in data sources, improvements in data analysis techniques, and evolution and upgrades in numerical models have tended to impart a temporal or "creeping" inhomogeneity into the real-time products of such centers. When the wind fields produced by these centers are used to drive a wave model, these creeping inhomogeneities are translated into the wave climate simulations. Therefore output data quality varies over time, and subtle changes in climate may be masked. Such deficiencies in real-time analyses have led major centers to major attempts to produce a consistent analysis of the atmosphere through so-called "reanalysis" using historical atmospheric observations and current analysis schemes and NWP models. A preliminary global atmospheric reanalysis produced at the ECMWF for the 15 year period 1979–1993 was used by *Sterl et al.* [1998] to make a global wave hindcast using the 3G WAM model. While the wave hindcast was found to underestimate high winds and sea states, the bias in MMSWH (about 5%) was considered low enough to use the hindcast to form a 15 year climatology of global waves and to analyze for trends. However, Sterl et al. were unable to confirm a significant change in the global wave climate within such a short hindcast period.

NWP centers have continued with major reanalysis projects. The first of these projects to be completed is the NCEP/National Center for Atmospheric Research (NCAR) Reanalysis (NRA) [*Kalnay et al.*, 1996], which spans a full 40 year period, 1958–1997. The study reported here is based upon the products of the first 40 year global wave simulation to be driven by the global surface marine wind fields produced by the NRA products, which is henceforth referred to as the Global Reanalysis of Ocean Waves (GROW). GROW was carried out by Oceanweather Inc. using a deep water version of its proven Ocean Data Gathering Program version 2 (ODGP2) spectral ocean wave model. GROW therefore is the first truly long-term multidecadal global wave hindcast based upon reanalysis wind fields that are at least produced in a homogeneous fashion. The main objectives of this paper are to document the GROW methodology, to establish the accuracy of the wave height hindcast, and to present the first-order results with regard to global significant wave height (SWH) wave climate and global trend patterns as by *Sterl et al.* [1998] but based on a more recent 40 year reanalysis.

This paper is organized as follows. Section 2 describes the wave model used and the basic hindcast methodology used. Section 3 describes the in situ and satellite-measured wind speed and wave height data sets used to evaluate the hindcast skill over as long an historical period as possible, as described in section 4. Section 5 gives the results of our analysis of wave height climate trend and variability, and Section 6 gives our conclusions.

2. Wave Hindcast Methodology

2.1. Source Wind Fields

The wind fields used in the generation of the wave hindcast were the NRA 6 hourly 10 m wind fields. In the NRA, buoy and ship winds were assimilated at an assumed reference level of 10 m [*Kalnay et al.*, 1996] regardless of the actual height of the measurement (buoy winds are usually measured at 5 m, while ship and platform observations range from about 15 m to more than 100 m). Satellite winds were not assimilated into the NRA product and are therefore the only truly independent set of wind speeds available for validation of the NRA wind fields.

The only adjustment made to the original NRA wind fields for this hindcast was an adjustment to neutral stability, using the technique described by *Cardone et al.* [1990]. The stability information required by that technique was derived from the NRA 2 m temperature and sea surface temperature fields. The neutrally stable NRA wind fields were previously evaluated by *Swail and Cox* [2000] and found to produce very good wave hindcasts for the North Atlantic when compared to buoy wave measurements (bias: hindcast-measured of −0.03 m; scatter index of 0.26) and satellite altimeter wave measurements (bias: hindcast-measured of −0.18 m, scatter index of 0.23).

2.2. Wave Model

The GROW wave model consists of the deep water ODGP2 spectral growth dissipation algorithm coupled with a global wave propagation system with great circle propagation effects included [*Greenwood et al.*, 1985]. This combination is substantially the same as that adopted by FNMOC in their Global Spectral Ocean Wave Model (GSOWM) model. The propagation scheme is rigorously energy conserving and has been shown in a recent study [*Cardone et al.*, 1995] to propagate accurately low-frequency swell over thousands of miles. The spectrum is resolved in 24 directional bins (15° angular bandwidth) and 23 frequency bins ($Df/f = .01$).

For GROW, the ODGP2 wave model is adapted on a global grid spacing of 1.25° in latitude by 2.5° in longitude. Most marginal seas are resolved, though smaller bays and straits such as Gibraltar and Malacca are not resolved.

In the model integration, wind fields are updated at 6 hourly intervals, and the model time step is 3 hours. Output wind and wave fields are archived at 6 hourly intervals at all model grid points, while directional spectra are archived at 6 hourly intervals every 10° of latitude and longitude. The ice field was specified on a monthly basis, using long-term mean monthly historical ice concentration data. Grid points at which the ice concentration is five tenths or greater are treated as land.

ODGP2 consists of an updated version of the ODGP source term formulation first described by *Cardone et al.* [1976]. ODGP treats the source terms of growth and dissipation in the manner of a first generation (1G) model, while ODGP2 raised the source term formulation to 2G standards as described in detail most recently by *Khandekar et al.* [1994]. The skill of this model has also been documented in numerous studies, most recently by *Cardone et al.* [1996] and *Cardone and Resio* [1998]. In fact, these recent studies indicate that the recent 3G for-

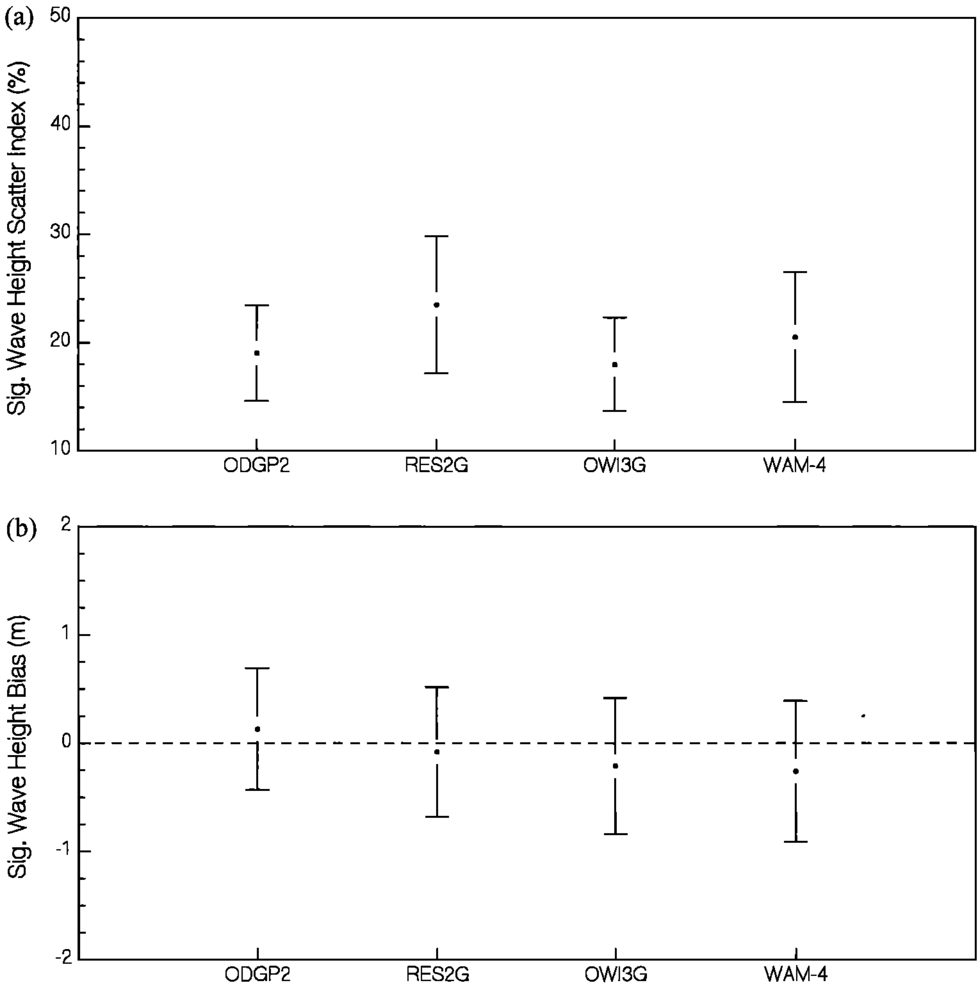

Figure 1. Relative performance of the ODGP2 model used in this study against contemporary 2G and 3G wave models in the two events evaluated by *Cardone et al.* [1996]. (a) The SWH scatter index and (b) over all comparisons at eight deep water data buoys (a total of 1010 data pair in both events). The vertical bars represent the standard deviation of the difference measure computed over the distinct buoy/storm data sets and therefore provides a measure of the consistency of model skill.

mulations provide no discernable increase in skill in specification of SWH over that of ODGP2 in both tropical and extratropical regimes, even in extreme sea states up to SWH of 12 m.

Figure 1 summarizes the comparative skill of four models evaluated by *Cardone et al.* [1996] against SWH time series at eight deep water buoys moored off the east coast of North America in two very severe storms. Figure 1a shows the scatter index for each model computed over 1010 hindcast measurement data pairs, while the vertical bars represent the standard deviation of the scatter index over all the individual buoy comparisons (i.e., 16 data sets representing eight buoys in two storms), thereby providing a measure of the consistency of the skill from buoy to buoy and storm to storm. Figure 1b gives the average skill and its variation in terms of mean differences.

Above on SWH of about 12 m all models tended to underspecify peak storm SWH, though the bias is slightly lower for 3G than 2G models. However, it should be noted that for the purpose of GROW any deficiency of hindcasts for such rare extreme storm seas should not affect the quality of the hindcast or the wave height climate statistics analyzed in this paper with regard to global wave climate, its variability, and its trend. First, as shown by *Cardone et al.* [1996], regardless of the model used, the specification of peak sea states in the most extreme events (SWH > 12 m) requires very accurate specification of very high winds in surface wind jet streaks. These are not resolved even in reanalysis wind products. Therefore we do not claim, nor do we recommend, that long-term continuous hindcasts based on reanalysis products be used for derivation of extreme event design criteria (e.g., 100 year return period maximum wave heights). Second, the upper limit of the SWH distribution analyzed in this paper from GROW, namely, the 99th percentile is about 9 m even in the harshest wave climate (see Plate 4, discussed in section 5), and this is well within the range of demonstrated accuracy of the ODGP2 model, in general, and of the GROW hindcast, specifically, as validated in this paper.

3. Validation Data

3.1. In Situ Data

3.1.1. Buoys and platforms. The in situ validation data set included 40 buoys, measurement platforms, and ocean weather stations mainly located in the Northern Hemisphere

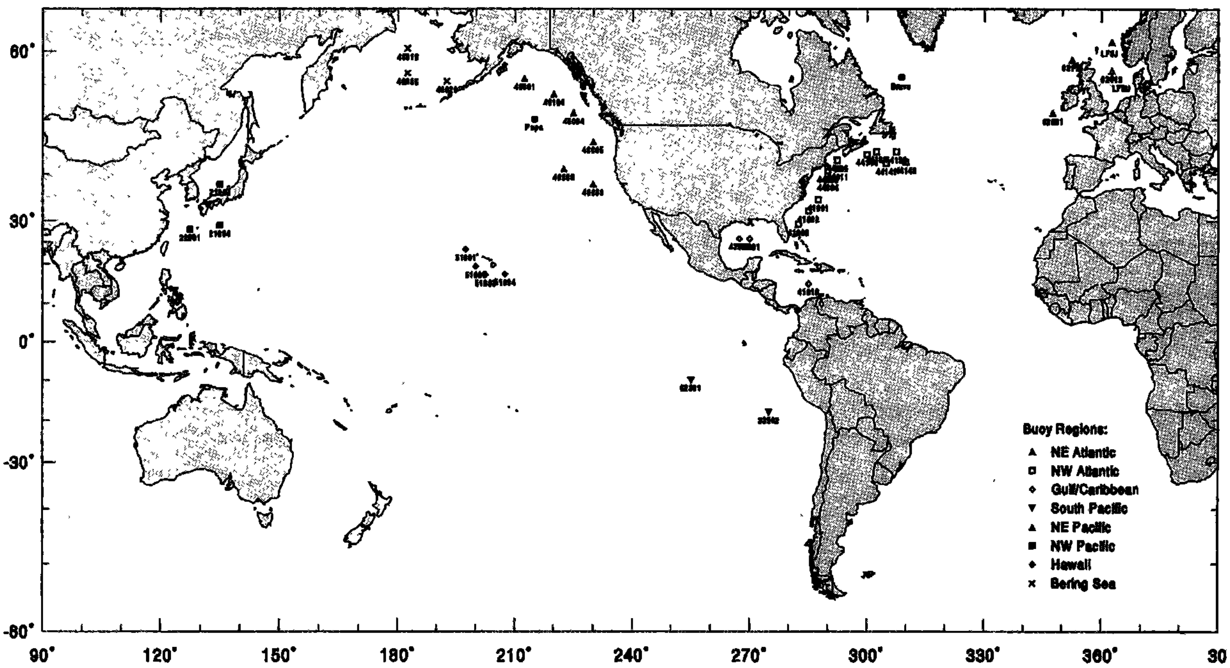

Figure 2. In situ data locations with buoy/platforms by region.

along the continental margins (Figure 2). The in situ measured wind and wave data came from a variety of sources. U.S. buoy data came from the National Oceanic and Atmospheric Administration (NOAA) Marine Environmental Buoy Database on CD-ROM; the Canadian buoy data came from the Marine Environmental Data Service marine CD-ROM; the remaining buoy and platform data (notably, the northeast Atlantic and northwest Pacific regions) came from the Comprehensive Ocean-Atmosphere Data Set (COADS) described by *Slutz et al.* [1985]. Comparisons were restricted to well-exposed deep water sites with the longest records. The wave measurements are comprised of 20 min samples (except for Canadian buoys, which were 40 min) once per hour. The wind measurements were taken as 10 min samples, scalar-averaged, except vector-averaged at the Canadian buoys, also once per hour. The wind and wave values selected for comparison with the hindcast were the mean of three successive hourly values centered on each 6 hour synoptic time. All wind speeds were adjusted to 10 m neutral winds following the approach described by *Cardone et al.* [1990].

3.1.2. Ocean weather ships. Data from Ocean Weather Ship (OWS) *Papa* were obtained from the Environment Canada National Archive System. The data were all observed from one of two ship classes: prior to 1965 the ships occupying OWS *Papa* were the Stone Class frigates *Stonetown* and *Sainte Catherines*, with anemometer heights of 20 m; subsequently, observations were taken from the sister ships *Quadra* and *Vancouver*, with anemometer heights of 28 m. Data from OWS *Bravo* were obtained from the U.S. National Climatic Data Center. A large number of vessels occupied OWS *Bravo*; however, they tended to be one of two classes, with anemometer heights of 24 m.

3.2. Satellite Data

Altimeters from the ERS-1, ERS-2, and TOPEX instruments were used for global wind and wave comparisons. The ERS-1/2 altimeter data sets were obtained from the Ifremer CD-ROM data set, while TOPEX data (Geophysical Data Records (GDR) Generation-B CD-ROM set) were obtained from the NASA Physical Oceanography Distributed Active Archive Center at the Jet Propulsion Laboratory/California Institute of Technology. The ERS-1, ERS-2, and TOPEX data were extracted for the entire available period, which was August 1991 to June 1996, August 1995 to January 1998, and September 1992 to January 1998, respectively.

The altimeter data sets were decoded using the recommended quality controls described in the ERS-1, ERS-2, and TOPEX documentation. Further corrections and quality control measures were used as recommended by *Cotton and Carter* [1994] for each measurement platform to produce a combined data set that is consistent with buoy wind and wave measurements. Individual 1 Hz data points were then spatially averaged onto the wave model grid, and output were arranged onto the 6 hour synoptic times using a ±3 hour window.

4. Validation of Grow

4.1. Validation Against Buoy and Platform Measurements

Figure 3 shows a typical time series of wind speed and SWH for buoy 46006 in the northeastern Pacific Ocean. In general, both the GROW winds and waves track the buoy observations. When strong extratropical systems passed close to a measurement site, the very highest winds and waves tended to be somewhat underpredicted; typically, the lowest winds and waves tended to be slightly overpredicted.

Individual buoys and platforms were then grouped by region (Figure 2) for comparison. Table 1 shows regional grouped statistics and represents more than 500,000 wind and wave observations. Highest scatter indices (SI) are from the northwest Pacific and northeast Atlantic regions, which were made up exclusively of COADS data. The COADS data lack both the

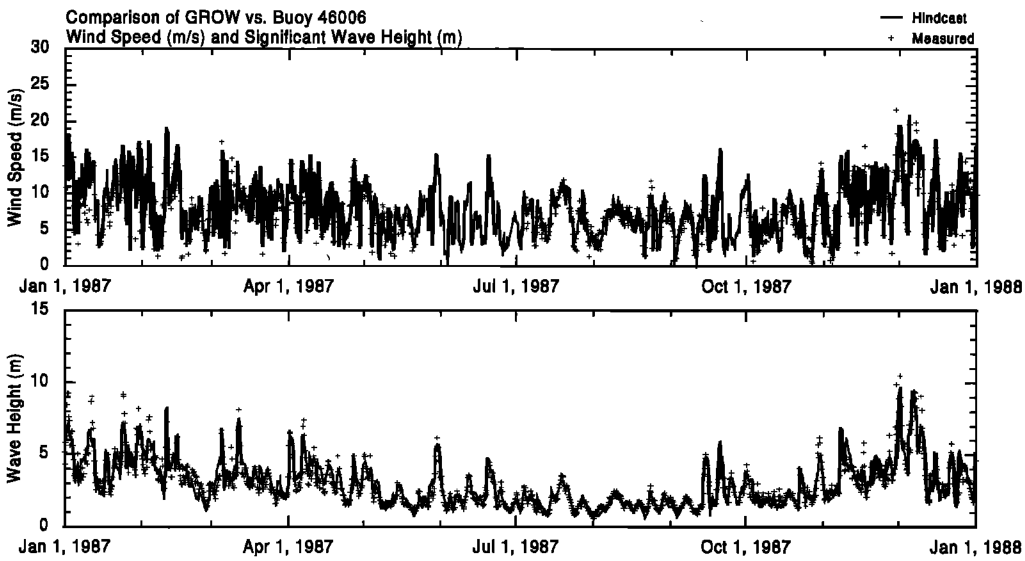

Figure 3. Comparison of GROW wind speed (m s^{-1}) and significant wave height (m) versus buoy 46006.

time resolution (3/6 hours versus 1 hour) and coding accuracy (winds nearest 1 knot, waves 0.5 m) than the other regions obtained from the CD-ROM marine data sets, which may explain some of the differences in SI. The Canadian and U.S. buoys were grouped into one data set since they represented the best science quality validation data set. These statistics show very good agreement with a mean bias of 0.12 m s^{-1} for winds and 0.10 m for waves and SI of 0.31 and 0.27, respectively.

Wind speed quantile-quantile (Q-Q) comparisons for the buoy and platforms by region (Figure 4) generally show good agreement outside of the tropics. There is some overestimation of the wind speeds in the 1st to 5th percentiles but good agreement up to the 99th percentile. The exception is the NW Pacific region, which consists of the 3 Japanese Meteorological Agency (JMA) buoys; this is considered to be due in large part to errors in the JMA buoy data available in COADS, which showed many unexplained large spikes and noise. They show the NRA underestimating the winds from the 25th to 99th percentiles. Wind comparisons in the three tropical buoy regions (Gulf/Caribbean, South Pacific, and Hawaii) show somewhat less agreement, which appears to be a characteristic of the NRA in tropical regions.

The Q-Q comparisons for significant wave height (Figure 5) again show good agreement for the midlatitude regions. The banding displayed in the NE Atlantic and NW Pacific regions is due to the coding accuracy available in COADS and the lack of hourly data for smoothing purposes. In general, the midlatitude regions show some overestimation in the 25th to 75th percentiles, but that is <0.5 m in the average of each COADS measurement band. Again, the NW Pacific buoys show more bias, particularly in the 50th percentile. In the Gulf/Caribbean region the wave heights are over estimated by GROW, which is consistent with the overestimation of wind speed. The opposite is true for the Hawaii region, where trade wind events are not properly modeled. In the South Pacific region, which mainly consists of buoy 32302, the wave heights are underestimated above the 50th percentile, even though wind speeds showed slight overestimation; this is primarily due to lack of swell arriving at the buoy location in GROW.

4.2. Validation Against Ocean Weather Stations

Figures 6 and 7 show a 1 year time series from OWS *Papa* (North Pacific) and *Bravo* (North Atlantic). The comparison tends to be more noisy than buoy comparisons but shows the same trend of GROW to underpredict the highest winds and sea states and slightly overpredict the lowest. Table 1 summarizes the statistics from both *Papa* and *Bravo*. Overall, the wind speed bias is −0.83 and −0.8 m s^{-1} and wave bias of 0.85 and 0.21 m for *Papa* and *Bravo*, respectively.

4.3. Validation Against Satellite Altimeter

Altimeter wind and wave measurements provide the best global spatial coverage to evaluate GROW and are an independent assessment since they were not assimilated in the NRA. Statistics and plots from the individual instruments (ERS-1, ERS-2, and TOPEX) showed very good agreement among each other, so the data sets were combined for these comparisons. The model comparison was broken into four regions: Southern Hemisphere (SH) (65°–20°S), Tropical (TROP) (20°S–20°N), Northern Hemisphere (NH) (20°–70°N), and all regions combined (65°S–70°N).

Q-Q plots of the combined altimeter versus GROW (Figure 8) show excellent agreement for both wind speed and wave height. Similar plots sorted by season (not shown) show similar results with no noticeable seasonal differences when global comparisons are made. Both the SH and TROP wave height comparisons show a slight trend of GROW to underestimate the wave height at higher sea states, while the NH waves show better agreement. Statistics for the same regions (Table 2) show that GROW and altimeter measurements agree very well with no wind speed bias and a wave height bias of 0.04 m overall.

The global coverage of the altimeter measurements made it possible to plot contours of wind and wave bias on a global projection. These plots were computed by taking all wind/wave measurement in a 5° box surrounding each grid point, calculating the bias, and then contouring the results. There were an average of 10,902 comparisons per 5° degree box. Any box with less than half the average was not plotted, which excluded

Table 1. Regional Statistical Comparisons of GROW Versus In Situ Buoy and Platform Observations[a]

	Number of Points	Mean Measurements	Mean Hindcasts	Difference (Hindcasts-Measurements)	Standard Deviation	Scatter Index	Correlation Coefficient
			Northeast Atlantic				
Wind Speed, m s^{-1}	30026	8.40	8.73	0.33	2.71	0.32	0.80
Wind Direction, deg	30032	243.06	238.06	−4.81	29.78	0.08	N/A
Significant Wave Height, m	24530	2.58	2.84	0.26	1.27	0.49	0.76
Northwest Atlantic							
Wind Speed, m s^{-1}	179938	7.14	7.54	0.40	2.54	0.36	0.78
Wind Direction, deg	179940	248.55	270.12	4.40	36.00	0.10	N/A
Significant Wave Height, m	175256	1.98	2.04	0.06	0.56	0.28	0.89
			Gulf of Mexico/Caribbean				
Wind Speed, m s^{-1}	59104	6.20	6.47	0.27	2.01	0.32	0.76
Wind Direction, deg	59104	101.09	90.47	−5.78	31.87	0.09	N/A
Significant Wave Height, m	55642	1.17	1.49	0.33	0.36	0.31	0.88
			South Pacific				
Wind Speed, m s^{-1}	12727	6.48	6.77	0.29	1.39	0.21	0.77
Wind Direction, deg	12727	122.71	125.27	2.60	19.21	0.05	N/A
Significant Wave Height, m	12607	2.14	1.82	−0.32	0.36	0.17	0.77
			Northeast Pacific				
Wind Speed, m s^{-1}	121323	7.99	8.04	0.05	2.26	0.28	0.82
Wind Direction, deg	121323	252.01	250.03	1.40	32.32	0.09	N/A
Significant Wave Height, m	121793	2.75	3.01	0.26	0.62	0.23	0.92
			Northwest Pacific				
Wind Speed, m s^{-1}	37893	7.44	6.72	−0.71	2.70	0.36	0.73
Wind Direction, deg	37896	357.96	4.58	−3.40	43.07	0.12	N/A
Significant Wave Height, m	29555	1.40	1.88	0.48	0.85	0.60	0.67
			Hawaii				
Wind Speed, m s^{-1}	70304	7.17	6.53	−0.64	1.74	0.24	0.74
Wind Direction, deg	70304	73.68	75.62	1.12	23.01	0.06	N/A
Significant Wave Height, m	69289	2.38	2.10	−0.29	0.42	0.17	0.82
			Bering Sea				
Wind Speed, m s^{-1}	19600	8.60	8.79	0.19	2.49	0.29	0.81
Wind Direction, deg	19601	34.99	42.84	−1.44	33.61	0.09	N/A
Significant Wave Height, m	16271	2.68	3.08	0.40	0.64	0.24	0.93
			Ocean Weather Ship Papa				
Wind Speed, m s^{-1}	33370	9.70	8.86	−0.83	2.72	0.28	0.80
Wind Direction, deg	33368	242.87	237.67	−3.05	28.57	0.08	N/A
Significant Wave Height, m	25571	2.54	3.39	0.85	1.10	0.43	0.76
			Ocean Weather Ship Bravo				
Wind Speed, m s^{-1}	21873	10.21	9.41	−0.80	2.99	0.29	0.78
Wind Direction, deg	21870	284.29	276.43	−1.43	32.34	0.09	N/A
Significant Wave Height, m	21583	2.95	3.16	0.21	1.02	0.34	0.81
			All Regions Combined (U.S. and Canadian Buoys Only)				
Wind Speed, m s^{-1}	466252	7.30	7.42	0.12	2.30	0.31	0.79
Wind Direction, deg	466258	107.88	94.02	1.41	32.40	0.09	N/A
Significant Wave Height, m	453750	2.18	2.28	0.10	0.58	0.27	0.90

[a]The statistical methods used here were defined by *Cardone et al.* [1990].

some of the comparisons north of 65°N and south of 65°S, where altimeter coverage is less.

Plate 1 shows the global wind speed bias for all the altimeter measurements. In general, it shows that GROW has very little wind speed bias across the entire globe. The plot of wave height bias (Plate 2) shows spatially coherent regions of GROW overestimating and underestimating the measured waves. Many of the regions, such as the Caribbean Sea, Aleutian Island Chain, and North Sea, are suspected to be resolution effects of the GROW wave model as the grid spacing is too coarse to resolve the coastline. The large region of bias off Antarctica is suspected to be the effects of using mean monthly ice tables for the entire hindcast, the well-known problems with the NRA in this region due to incorrect assimilation of the Southern Hemisphere surface pressure input data (PAOBS) observations and a general lack of data in the area. There appears to be a large area of underestimation of wave height in the Southern Hemisphere along 30°S, with the strongest bias in the southeast Pacific. Analyses of wave height bias by season (not shown) generally show the same underestimation in the South Pacific and overestimation near the ice and land edges, with little seasonal difference.

Comparison of the global bias plots from the altimeter to the bias statistics generated from the buoy and platform measurements show excellent agreement in the sign and magnitude of the bias of GROW. Figure 9 shows a direct comparison between buoy 32002 and the combined altimeter measurements in an area where the hindcast is biased low relative to the

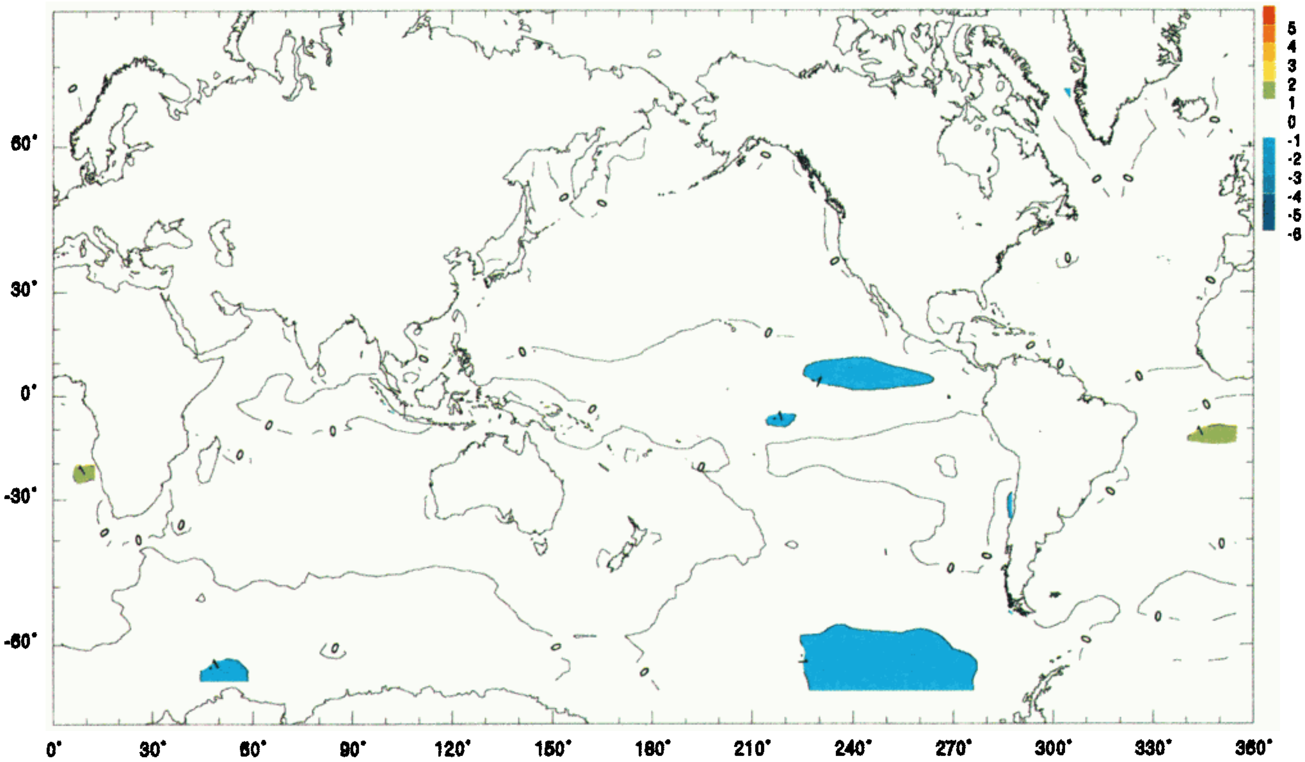

Plate 1. Mean difference of wind speed (m s^{-1}) between GROW and altimeter measurements (GROW-Altimeter).

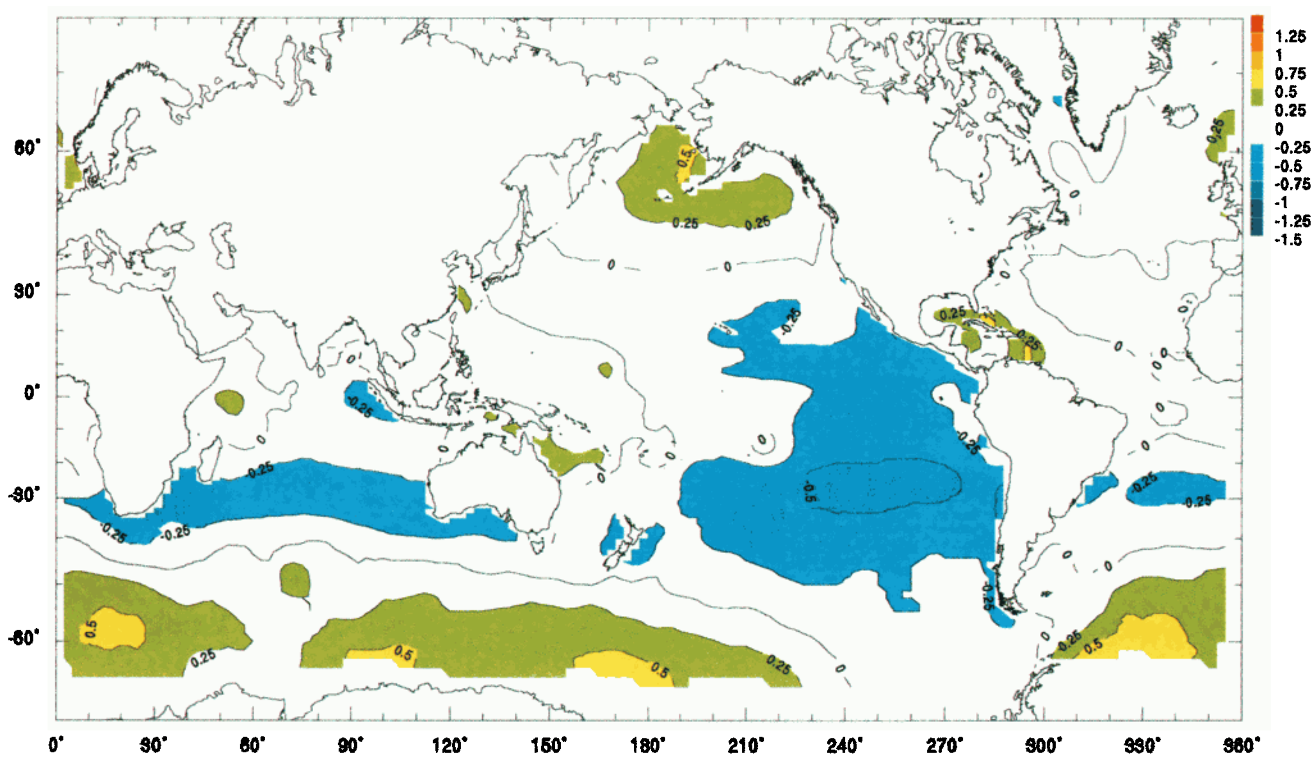

Plate 2. Mean difference of wave height (m) between GROW and altimeter measurements (GROW-Altimeter).

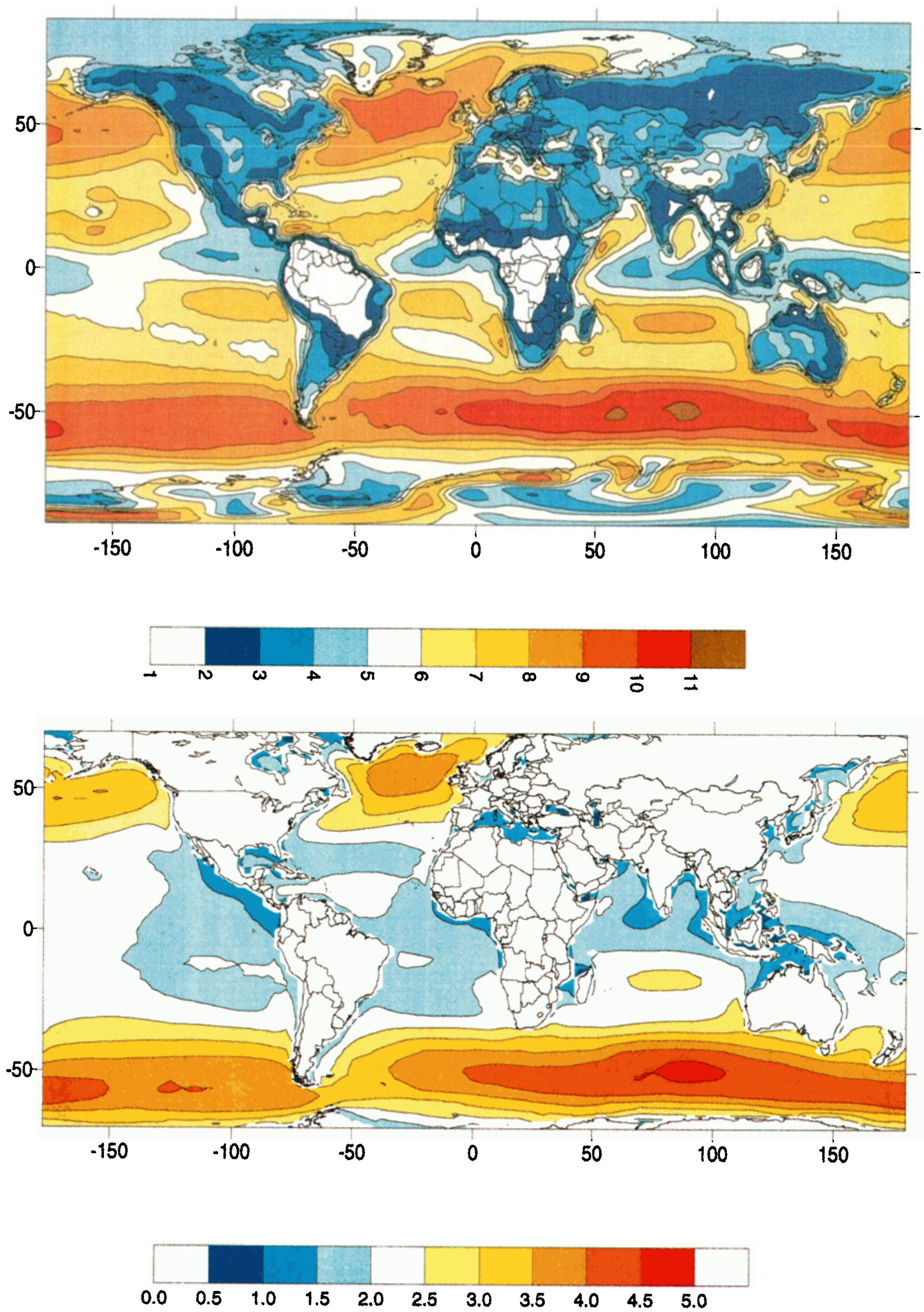

Plate 3. (top) Mean annual wind speed and (bottom) wave height.

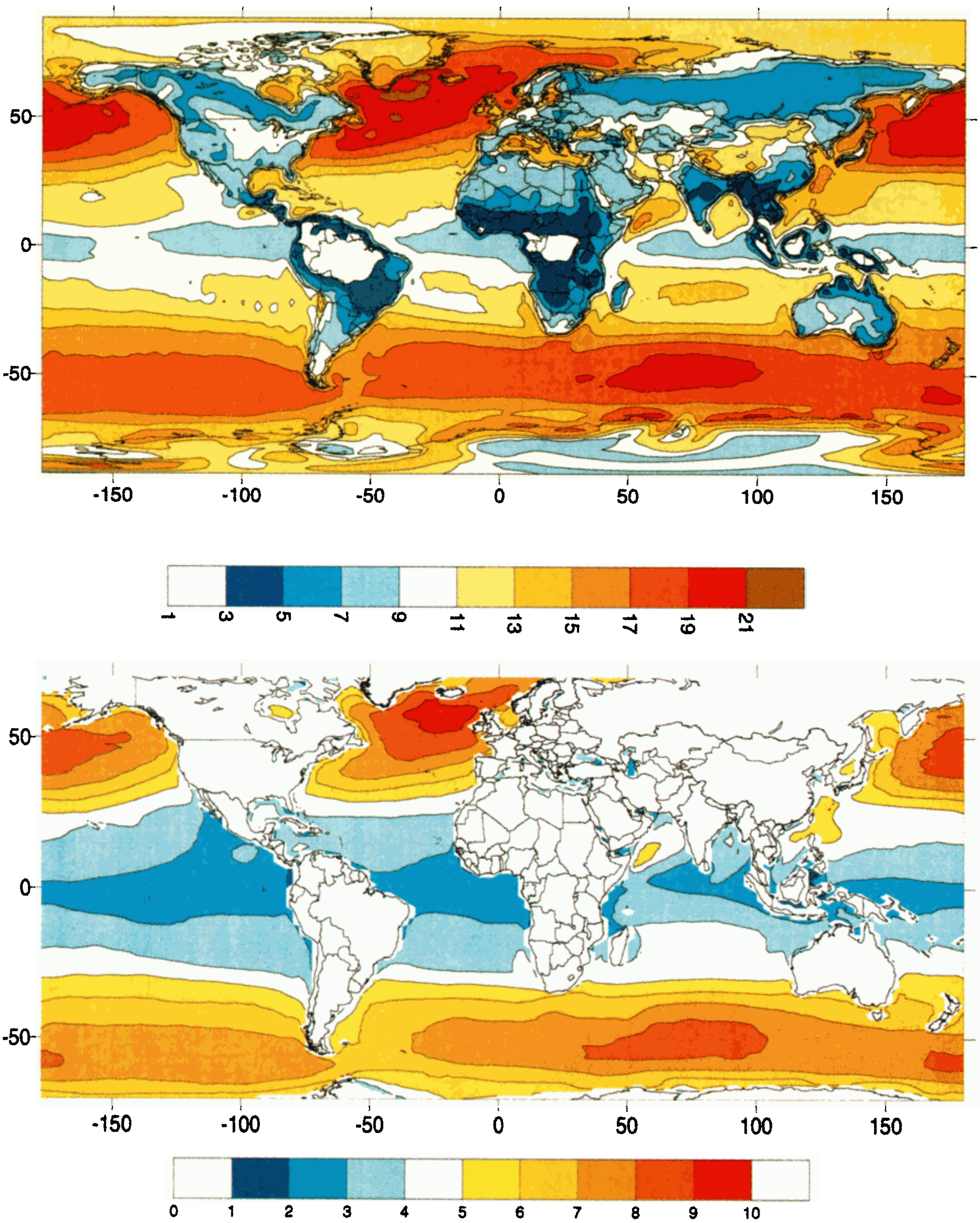

Plate 4. (top) Ninety-ninth percentile annual wind speed and (bottom) wave height.

anemometer. This confirms that the buoy measurements and the altimeter measurements are consistent; therefore this would tend to indicate that the small bias seen in other (mainly tropical) areas (other than near ice or land edges) is related to characteristics in GROW (e.g., swell) and not in the altimeter data sets. Still, it is noteworthy that these biases are <0.25 m in both Northern and Southern Hemisphere midlatitudes.

4.4. Summary of Validation Results

In summary, the global comparisons of available buoy, platform, ship, and altimeter data show excellent agreement in bias and scatter with GROW. Comparison of GROW and global altimeter measurements shows a zero wind speed and a −4 cm wave bias overall, with excellent agreement up to and including the 99th percentile. Intercomparison of buoy/platform results

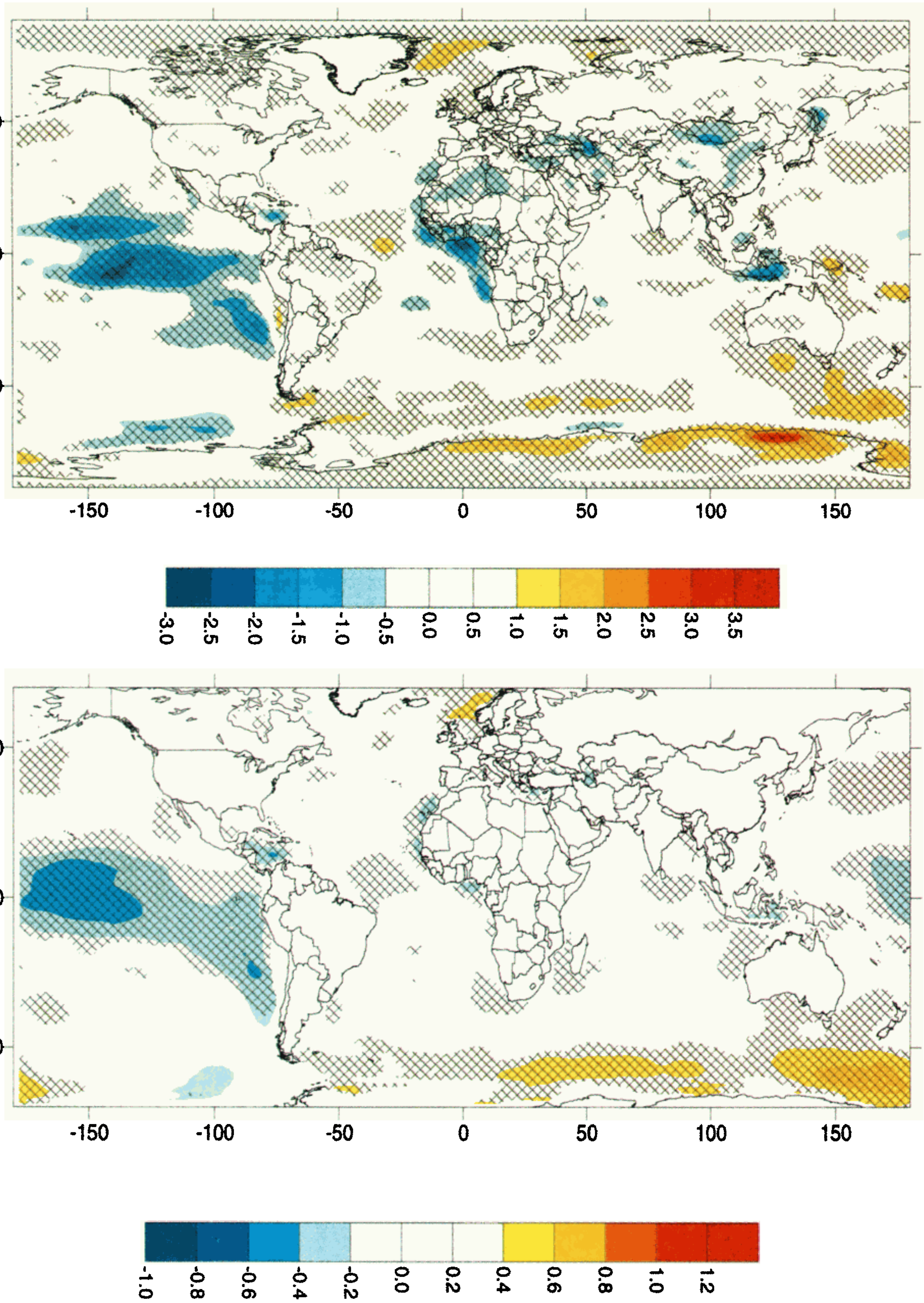

Plate 5. (top) Inferred change in mean annual wind speed and (bottom) wave height 1958–1997 with 99% statistical significance.

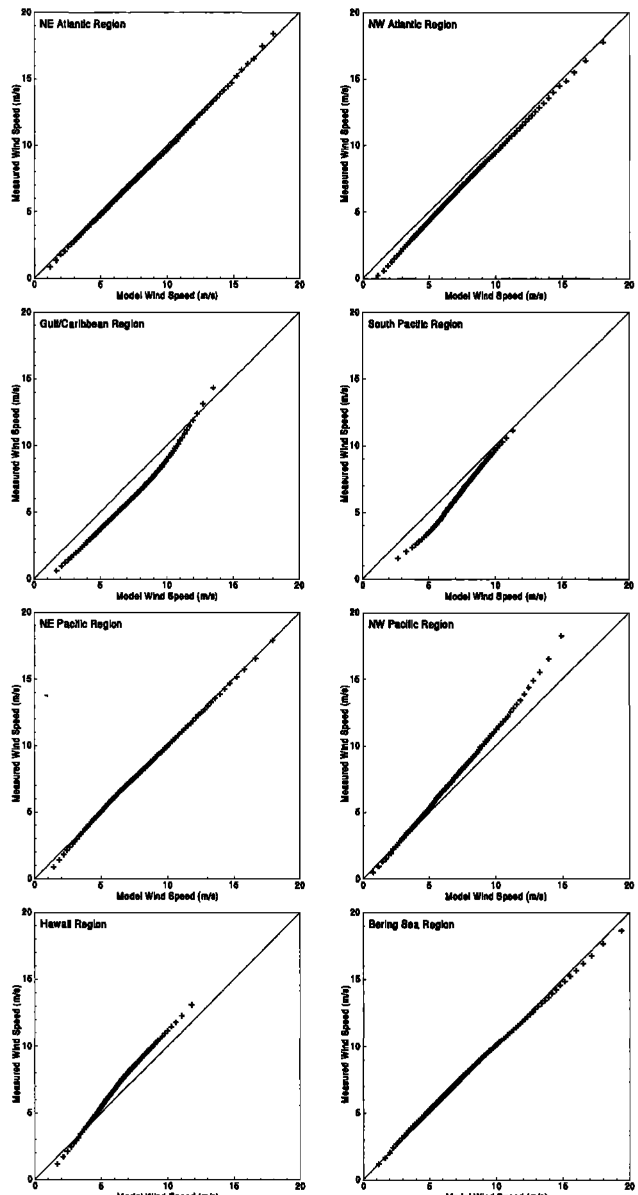

Figure 4. Q-Q plots (from 1 to 99%) for buoy/platform wind speeds (m s^{-1}) by region.

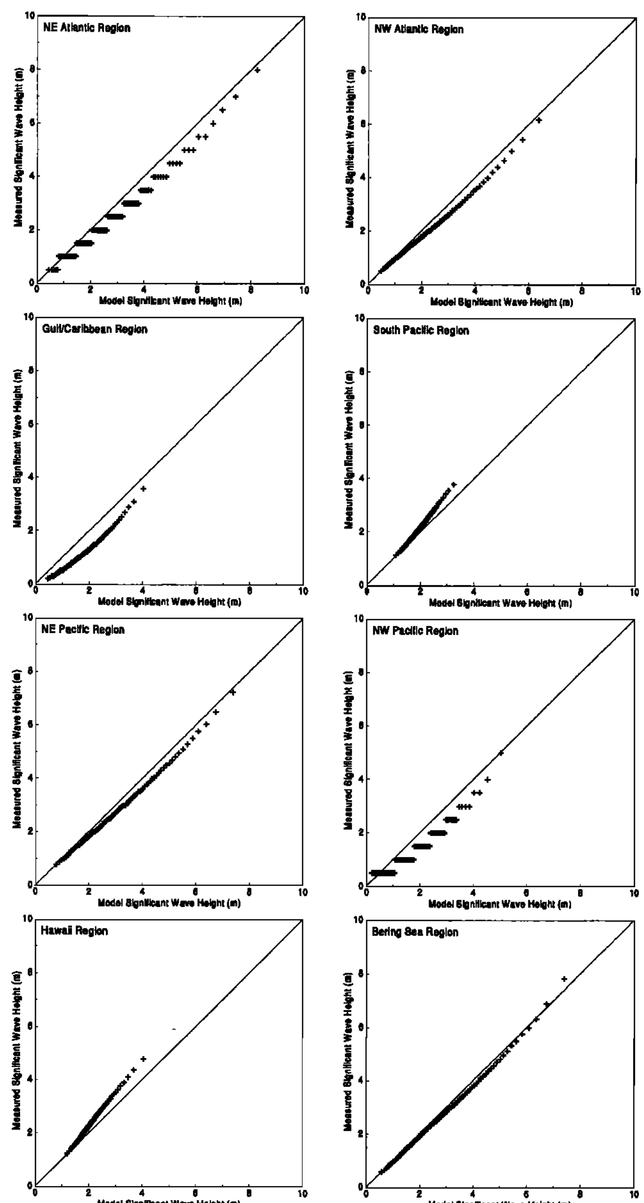

Figure 5. Q-Q plots (from 1 to 99%) for buoy/platform significant wave heights (m) by region.

and altimeter results shows that the two data sets are consistent with their assessment of the skill of GROW, with the exception of the NW Pacific region. As our review of the JMA buoy data available in COADS showed, there were many unexplained spikes and noise in the buoy data and the altimeter measurements are felt to be more reliable in this region. There is a tendency of GROW, as shown in the buoy comparisons, to overpredict slightly the lowest sea states in the midlatitudes; this tendency is similar to that found by *Sterl et al.* [1998] in their 15 year global wave hindcast using the ECMWF reanalysis winds.

5. Analysis of Climate Trend and Variability

Fifteen statistics were computed for both the resultant wave heights and the input wind fields on monthly, seasonal, and annual timescales; trend and variability analysis was carried out for each grid point in the global hindcast.

Plate 3 shows the global mean annual wind speed and wave height distribution for the period 1958–1997. The maxima in the high-latitude areas in both hemispheres and along the prevailing storm tracks are very evident in these charts. It is interesting to note that wind speeds over the land are far less than those over the oceans. As found by *Sterl et al.* [1998], the waves in the North Atlantic are higher than those in the North Pacific.

Plate 4 shows the geographical distribution of the annual 99th percentile wind speed and wave height for 1958–1997. The patterns are very similar to those for the means, although the areas of highest wind speed and wave height are even more accentuated. The areas of strongest winds are between Iceland and Canada, while in the mean charts the Southern Ocean showed higher values. The 99th percentile wind and wave charts do not reflect areas where episodic high winds and waves might be expected because of tropical storms, such as

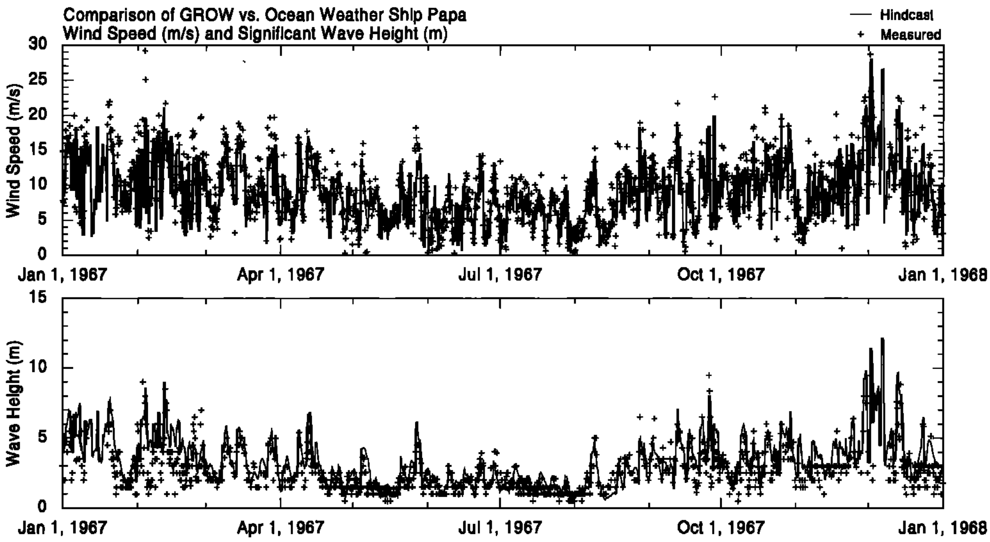

Figure 6. Comparison of GROW wind speed (m s^{-1}) and significant wave height (m) versus OWS *Papa*.

the southeastern U.S. coast and Gulf of Mexico, South China Sea, north Australia, or the Indian Ocean. This is certainly due to the inability, described earlier, of the NRA to resolve adequately these relatively small atmospheric features.

A statistical analysis of the trends in means and 99th percentile winds and waves was carried out at each point on the grid. Trends were computed as simple linear trends over the 40 years of the GROW hindcast using least squares fitting techniques; 99% statistical significance levels were also computed. Plate 5 shows the global trends in mean wind speed and significant wave height. Increasing trends are most noticeable in the northeast Atlantic Ocean, across the northern edge of the north Pacific Ocean, and along the margins of Antarctica. The Antarctic trends are considered to be rather unreliable because of the data scarcity in the Southern Ocean as a whole and documented problems in the NRA with the Southern Hemisphere, particularly south of 50°S. Negative trends in wind speed and wave height are found mostly in equatorial regions, particularly in the Pacific Ocean.

Plate 6 shows the global trends in the 99th percentile wind speed and wave height. The patterns show similar patterns to the mean trend charts, except that the trends are much more dramatic. The northeast Atlantic Ocean remains an area of noticeable increase in winds and waves, while the North Pacific trends are stronger at the western edge. In the Norwegian Sea the 99th percentile annual wave height has risen by more than 1 m over the 40 year period. The Southern Ocean shows strong increasing trends in some areas, decreasing in others; as noted above, these trends are not considered particularly reliable. Particularly noticeable in the wave height chart is the bipolar nature of the trends in the North Atlantic, with strong increases in the northeast and strong decreases in the south-central North Atlantic. This pattern closely resembles the one found by *Kushnir et al.* [1997], which they found follows the dominant mode of the NAO.

Analyses of seasonal trends were also carried out (not shown). The winter patterns were the most interesting and

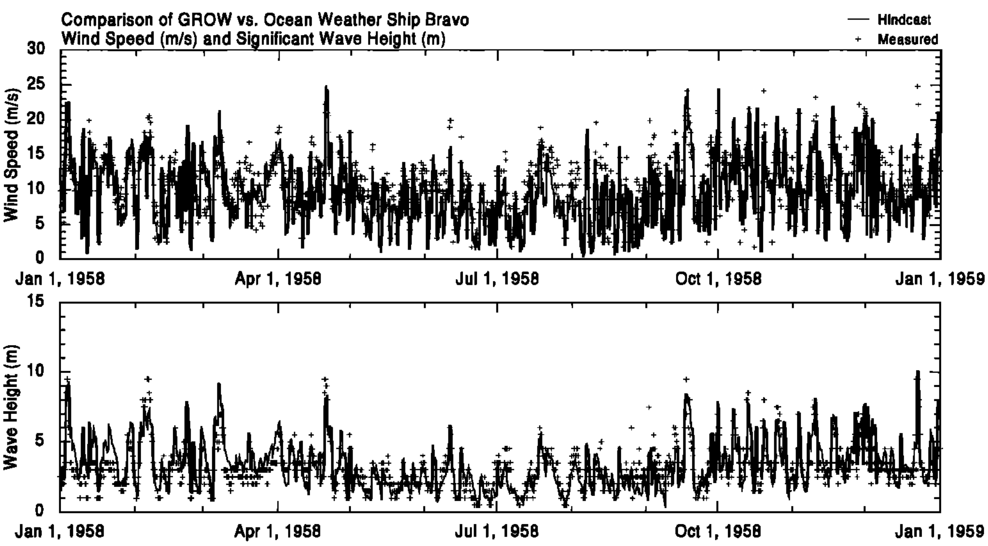

Figure 7. Comparison of GROW wind speed (m s^{-1}) and significant wave height (m) versus OWS *Bravo*.

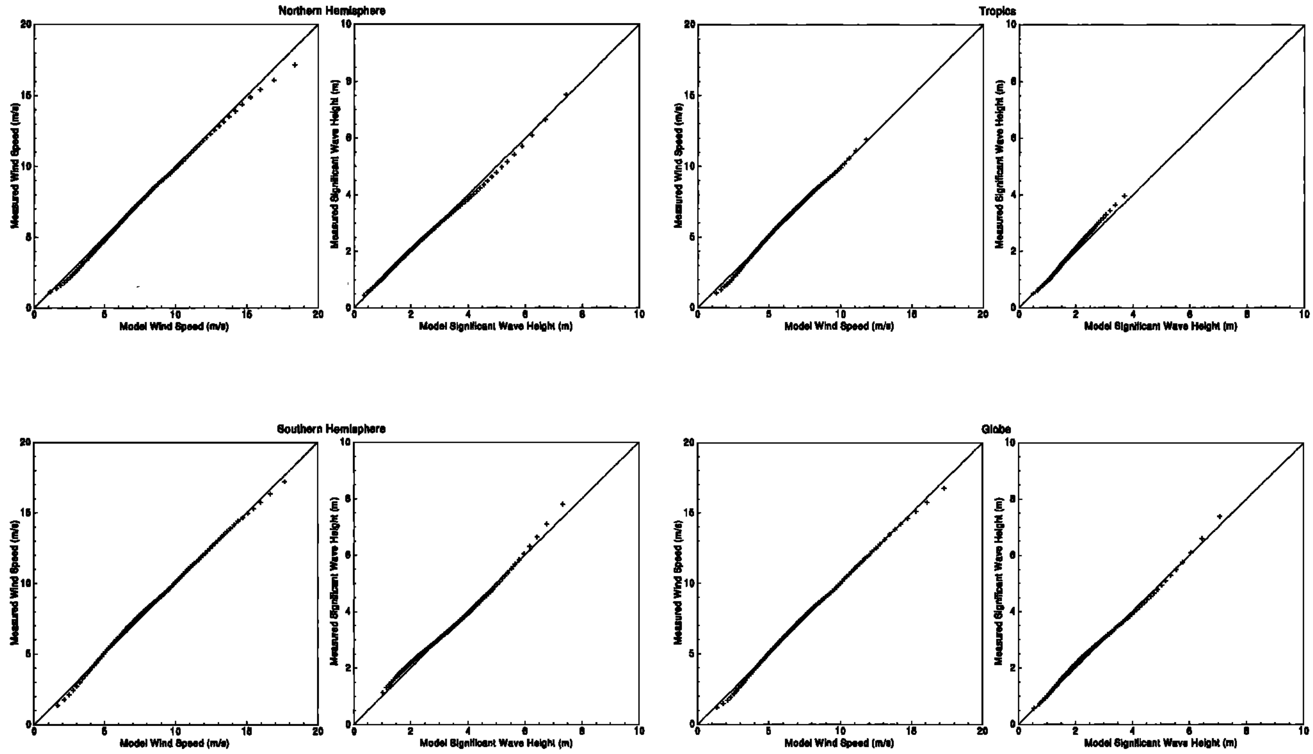

Figure 8. Q-Q (from 1 to 99%) wind speed (m s^{-1}) and wave height (m) comparisons of GROW and altimeter measurements for Northern Hemisphere (20°–70°N), Tropics (20°S–20°N), Southern Hemisphere (65°–20°S), and full globe.

dramatic, showing the same patterns as the annual analyses, although with more pronounced trends.

6. Discussion and Conclusions

This study describes the generation of the first 40 year global wave simulation driven by the NRA global surface wind fields. Extensive validation against in situ buoys, platforms, weather ships, and satellite altimeter measurements showed very good agreement with GROW not only in terms of bias and scatter but over the entire frequency distribution out to and beyond the 99th percentiles of both winds and waves. However, some regional biases can be found along ice/land edges and in the tropics, particularly in the Southern Oceans. While we would not recommend the direct use of the wind and wave data in the analysis of long return period statistics, there is no problem with its utility in assessment of wave climate, its trend, and its variability out to the 99th percentile.

The global trend analysis showed statistically significant areas of both increasing and decreasing winds and waves. The increasing trend in the northeast Atlantic and decreasing trend in the central North Atlantic are particularly well defined and consistent with changes reported in previous studies, which were linked to reported changes in the NAO. We have low confidence in the rather large trends found in parts of the Southern Ocean.

Table 2. Regional Statistical Comparisons of GROW Versus Altimeter Measurements[a]

	Number of Points	Mean Measurements	Mean Hindcasts	Difference (Hindcasts-Measurements)	Standard Deviation	Scatter Index	Correlation Coefficients
			Southern Hemisphere (65°–20°S)				
Wind Speed, m s^{-1}	4,004,211	8.68	8.62	−0.06	2.40	0.28	0.79
Significant Wave Height, m	4,001,377	3.39	3.34	−0.05	0.79	0.23	0.85
			Tropics (20°S–20°N)				
Wind Speed, m s^{-1}	2,608,601	6.02	5.99	−0.03	1.86	0.31	0.71
Significant Wave Height, m	2,593,660	1.96	1.87	−0.08	0.45	0.23	0.77
			Northern Hemisphere (20°–70°N)				
Wind Speed, m s^{-1}	2,086,601	7.43	7.60	0.18	2.08	0.28	0.84
Significant Wave Height, m	2,067,467	2.54	2.56	0.02	0.65	0.26	0.91
			All Regions Combined				
Wind Speed, m s^{-1}	8,699,413	7.60	7.60	0.00	2.18	0.29	0.81
Significant Wave Height, m	8,662,504	2.77	2.73	−0.04	0.67	0.24	0.89

[a]Statistical methods used here are defined by *Cardone et al.* [1990].

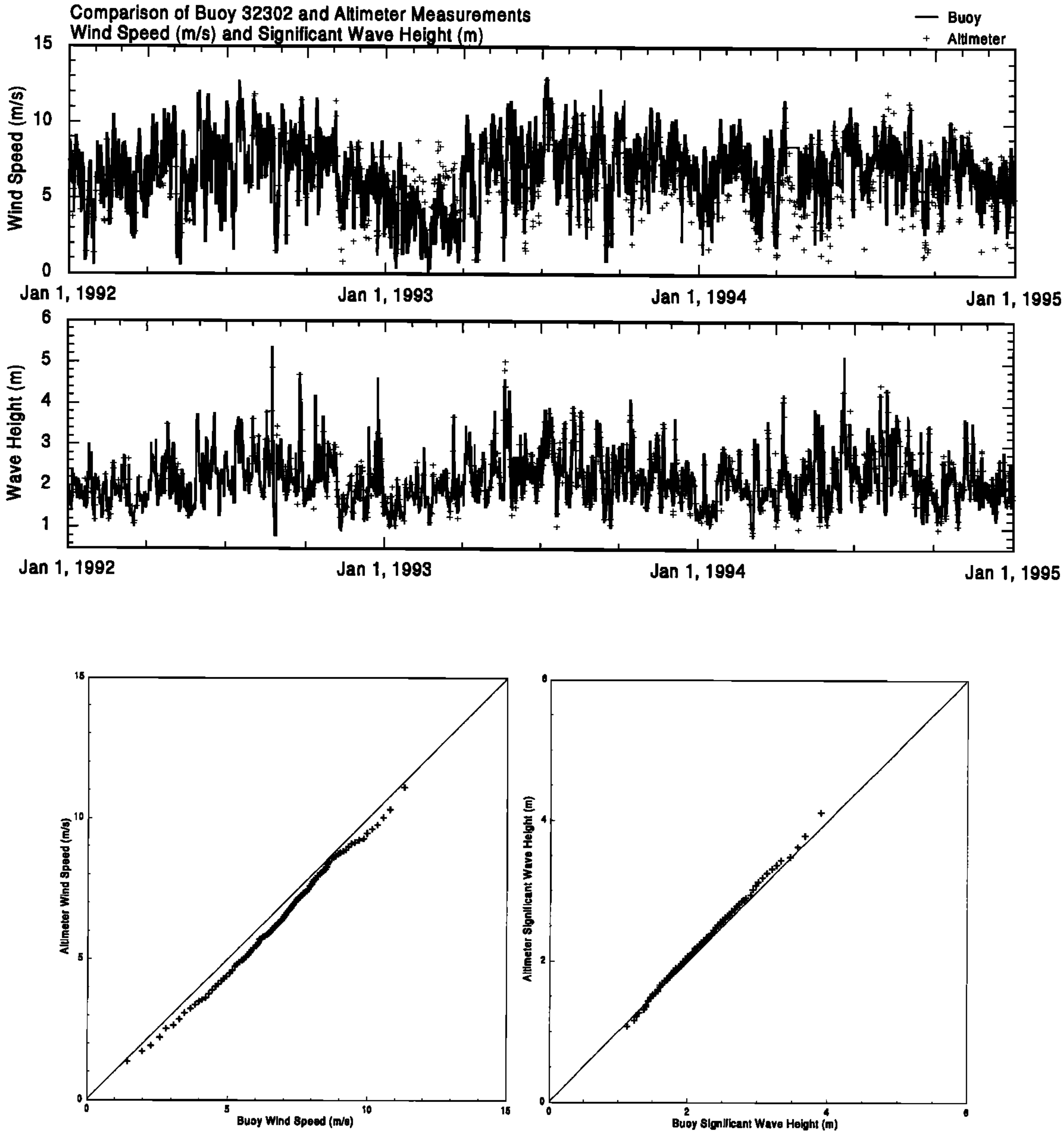

Figure 9. Intercomparison of buoy 32302 and altimeter measurements: wind speed (m s^{-1}) and wave height (m) time series (above) and Q-Q (from 1 to 99%) plots (below).

The trends described in section 5 are based on the NRA-driven GROW hindcast. While the NRA used the same numerical prediction scheme for the 40 year period, thus removing the bias associated with ever changing operational models, there still remain probable biases due to "creeping inhomogeneities." Numerous studies [*WASA Group*, 1998; *Schmidt and von Storch*, 1993; *von Storch and Zwiers*, 1999] have noted the difficulty in assessing the homogeneity of the observational record, both in terms of local observations and the number and quality of observations used in developing analyzed products. For ocean areas a documented increase in shipboard anemometer heights coupled with an increased fraction of measured versus estimated winds [e.g., *Kent and Taylor*, 1997] will contribute to an artificial increase in ocean winds. This effect was well demonstrated by *Cardone et al.* [1990]. These creeping inhomogeneities are potentially serious constraints to any attempt to derive long-term trends. Therefore it is important to compare the trend analyses derived from the GROW hindcast against some long-time histories of homogeneous measured data at selected points. Unfortunately, there are very few such locations in the global ocean.

One location for which we do have reasonably homogeneous wind measurements over the 40 year period of the GROW hindcast is at Sable Island, just off the east coast of Canada. We are also able to analyze the surface atmospheric pressure record from Sable Island, along with records from two other sites in Nova Scotia (Halifax and Sydney), to compute pressure triangle wind records. As shown by *Schmidt and von Storch* [1993], the pressure triangle geostrophic winds are likely the least biased wind estimator available since inhomogeneities in pressure records are much less than for most atmospheric variables.

Plate 7 shows the relative magnitudes of the wind speed trends for the Sable Island area from GROW, Sable Island

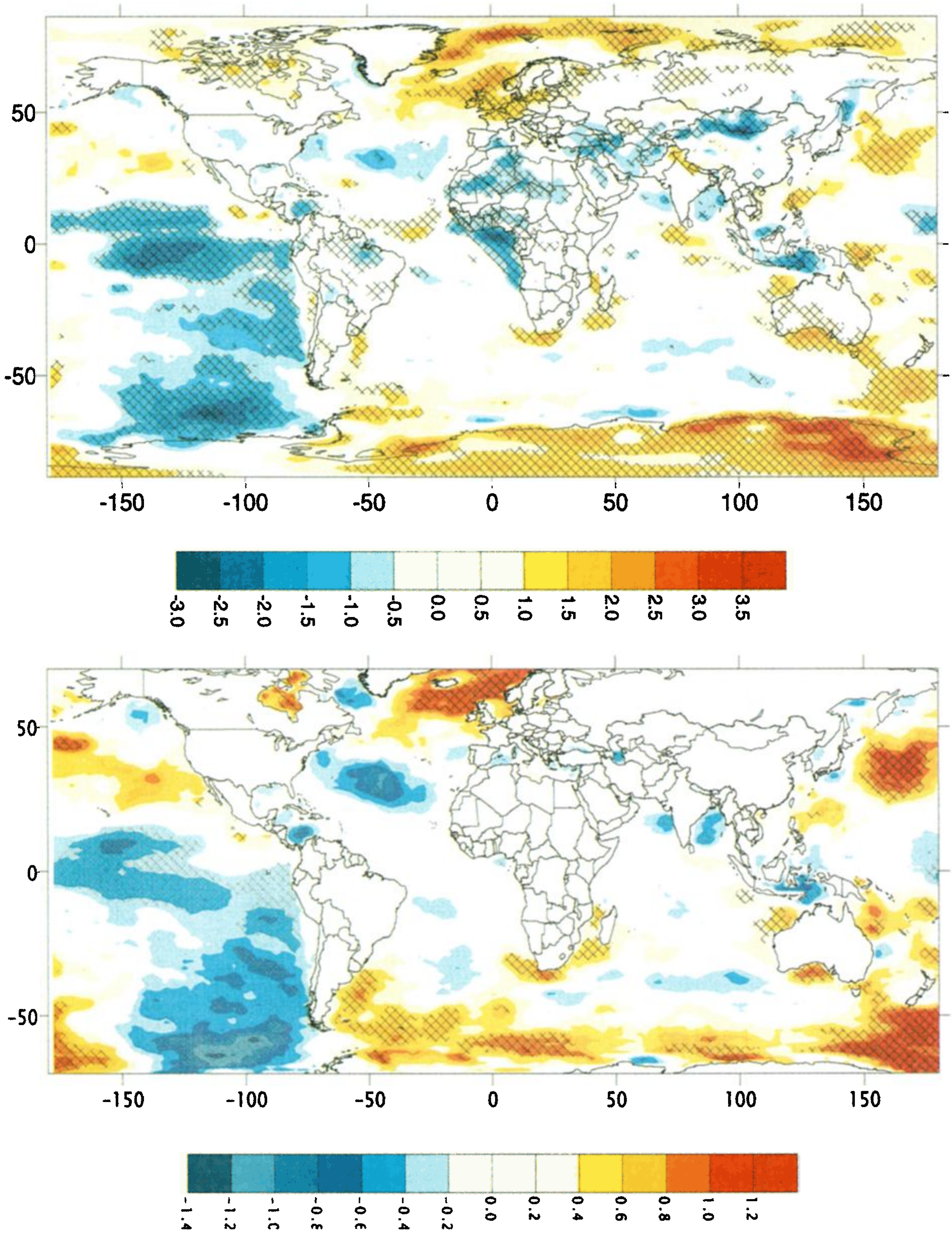

Plate 6. (top) Inferred change in 99th percentile wind speeds and (bottom) wave heights 1958–1997 with 99% statistical significance.

wind measurements, and the pressure triangle. In both the Sable Island measurements and the triangle winds the trends in the percentiles are decreasing. The magnitude of the decreasing trend is comparable for both the wind measurement and triangle analyses, with the triangle wind trend being slightly more negative. The GROW wind speed trends show a near-zero but very slightly positive trend. This apparent increase is likely artificial, the result of an inhomogeneity introduced into

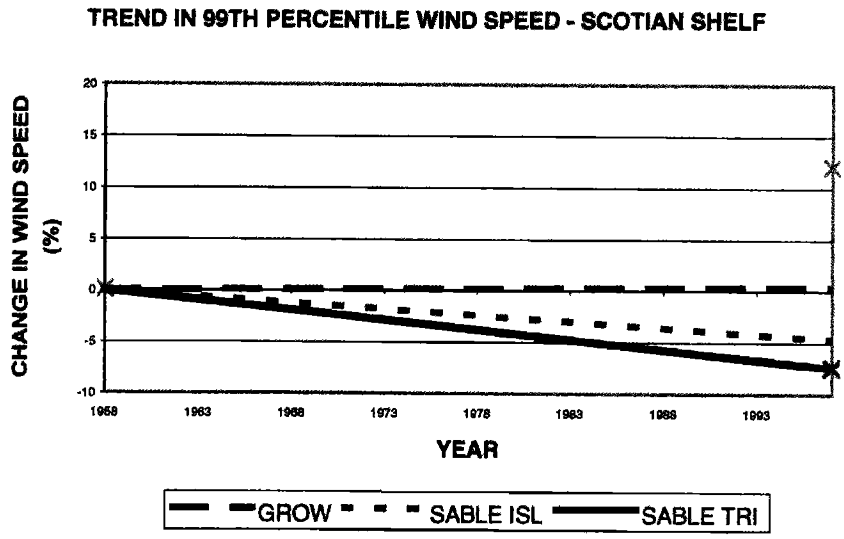

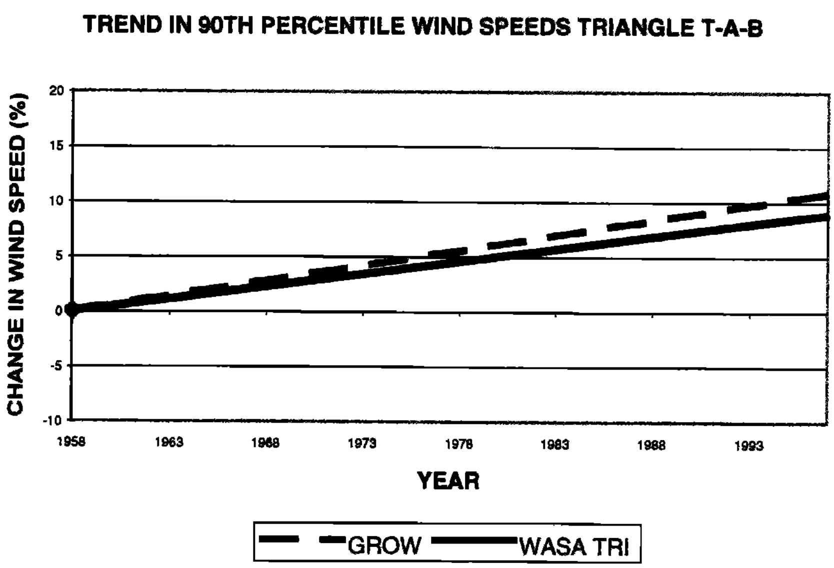

Plate 7. Trends in GROW wind speeds and corresponding point trends expressed as the inferred percent change in (top) 99th and (bottom) 90th percentile wind speed over the period 1958–1997 for the Sable Island area and the WASA triangle Thorshavn-Aberdeen-Bergen, respectively.

the NRA winds as described above. Ship winds are assimilated into the numerical models at an anemometer height of 10 m, when in fact the heights have increased from about 20 m at the beginning of the period to more than 30 m by the end of the period, with many recent observations coming from anemometers at heights exceeding 45 m. In the 1990s an increasing volume of moored buoy data would have been included in the NRA winds. These buoy winds are taken at 5 m height but also assimilated at 10 m into the model. By themselves the buoy winds would thus create an artificial negative bias. The actual bias seen here is a result of the combination of the positive bias due to the ships and the recent negative bias from the buoy. Both biases would be eliminated, or at least reduced, if all winds were assimilated at the correct heights.

A second area for which "ground truth" information is available for trends is off the Norwegian coast. *WASA Group* [1998] computed winds from the pressure triangle Thorshavn-Aberdeen-Bergen. Plate 7 shows the comparative results of the GROW hindcast and the WASA triangle. In this area the trend is strongly positive, with the GROW winds being slightly more positive than the triangle. This indicates that the GROW trends are reasonable, but probably slightly too high, or a good upper bound on real trends.

Comparisons with earlier wave trend analysis showed generally similar results, although much of the previous work was done on very limited sets of data, usually <20 years. *Bacon and Carter* [1991] show similar trends to those computed in this study for OWSs *India*, *Juliett and Lima*, and *Seven Stones* but with much greater magnitudes. They reported an increase of about 0.5 m in 24 years from 1962 to 1986 at *Seven Stones*; the GROW analysis had a 0.3 m increase over the same period.

In summary, the trend in wind speed and wave height produced from the GROW hindcast seem reasonable, at least as an upper bound on the true trends. The apparent creeping inhomogneities in the NRA winds highlight the need for additional investigation of the sources and magnitudes of the inhomogeneities by comparing the results of this (and subsequent) hindcasts to other long-term homogeneous data sets such as pressure triangles.

Acknowledgments. The analysis of GROW and the preparation of this paper was funded by the Canadian Federal Program of Energy Research and Development. The authors would like to express their sincere thanks to Ifremer and JPL for the provision of satellite altimeter data used in the wind and wave validation. We would also like to express our appreciation to Ain Niitsoo, who carried out the considerable processing of the climate statistics for the 18364 grid points. Last, we are deeply indebted to Vincent Cardone for his encouragement, support, and insight in the execution of this research and the preparation of this article.

References

Bacon, S., and D. J. T. Carter, Wave climate changes in the North Atlantic and North Sea, *Int. J. Clim.*, *11*, 545–558, 1991.

Cardone, V. J., and D. T. Resio, An assessment of wave modeling technology, paper presented at International Workshop on Wave Hindcasting and Forecasting, U.S. Army Eng. Waterw. Exp. Station, Melbourne, Fla., January 26–30, 1998.

Cardone, V. J., J. G. Greenwood, and M. A. Cane, On trends in historical marine wind data, *J. Clim.*, *3*, 113–127, 1990.

Cardone, V. J., H. C. Graber, R. E. Jensen, S. Hasselmann, and M. J. Caruso, In search of the true surface wind field in SWADE IOP-1: Ocean wave modelling perspective, *Global Ocean Atmos. Syst.*, *3*, 107–150, 1995.

Cardone, V. J., R. E. Jensen, D. T. Resio, V. R. Swail, and A. T. Cox, Evaluation of contemporary ocean wave models in rare extreme events: "Halloween Storm of October, 1991; Storm of the Century of March, 1993," *J. Atmos. Oceanic Technol.*, *13*, 198–230, 1996.

Corson, W. D., D. T. Resio, R. M. Brooks, B. A. Ebersole, R. E. Jensen, D. S. Ragsdale, and B. A. Tracy, Atlantic coast hindcast deepwater significant wave information, *WIS Rep. 2*, U.S. Army Eng. Waterw. Exp. Stn., Vicksburgs, Miss., 1981.

Cotton, P. D., and D. J. T. Carter, Cross calibration of TOPEX, ERS-1, and Geosat wave heights, *J. Geophys. Res.*, *99*, 25,025–25,033, 1994.

Eide, L. I., M. Reistad, and J. Guddal, Database for Computed Wind and Wave Parameters for the North Sea, Norwegian Sea, and Barents Sea Each 6-Hours for the Years 1955–1981, Norwegian Meteorol. Inst., Oslo, 1985.

Greenwood, J. A., V. J. Cardone, and L. M. Lawson, Intercomparison test version of the SAIL wave model, in *Ocean Wave Modelling*, pp. 221–233, Plenum, New York, 1985.

Gunther, H., W. Rosenthal, M. Stawarz, J. C. Carretero, M. Gomez, I. Lozano, O. Serano, and M. Reistad, The wave climate of the northeast Atlantic over the period 1955–1994: The WASA wave hindcast, *Global Atmos. Ocean Syst.*, *6*, 121–163, 1998.

Kalnay, E., et al., The NCEP/NCAR 40-year reanalysis project, Bull. *Am. Meteorol. Soc.*, *77*, 437–471, 1996.

Kent, E. C., and P. K. Taylor, Choice of a Beaufort equivalent scale, *J. Atmos. Oceanic. Technol.*, *14*, 228–242, 1997.

Khandekar, M. L., R. Lalbeharry, and V. J. Cardone, The performance of the Canadian Spectral Ocean Wave Model (CSOWM) during the Grand Banks ERS-1 SAR Wave Spectra Validation Experiment, Atmos. Ocean, *31*, 31–60, 1994.

Kushnir, Y., V. J. Cardone, J. G. Greenwood, and M. Cane, The recent increase in North Atlantic wave heights, *J. Clim.*, *10*, 2107–2113, 1997.

Schmidt, H., and H. von Storch, German bight storms analyzed, *Nature*, *365*, 791, 1993.

Slutz, R. J., S. J. Lubker, J. D. Hiscox, S. D. Woodruff, R. L. Jenne, D. H. Joseph, P. M. Steurer, and J. D. Elms, Comprehensive ocean-atmosphere data set release 1, NTIS PB86-105723, 268 pp., NOAA Environ. Res. Lab., Boulder, Colo., 1985.

Sterl, A., G. J. Komen, and P. D. Cotton, Fifteen years of global wave hindcasts using winds from the European Centre for Medium-Range Weather Forecasts reanalysis: Validating the reanalyzed winds and assessing the wave climate, *J. Geophys. Res.*, *103*, 5477–5492, 1998.

Swail, V. R., and A. T. Cox, On the use Of NCEP/NCAR reanalysis surface marine wind fields for a long term North Atlantic wave hindcast, *J. Atmos. Oceanic. Techn.*, *17*, 532–545, 2000.

U.S. Naval Oceanography Command, Hindcast spectral ocean wave model climatic atlas: North Atlantic Ocean, report, Nav. Oceanogr. Command Detachment, Asheville, N. C., 1983.

von Storch, H., and F. W. Zwiers, Statistical Analysis in Climate Research, 484 pp., Cambridge Univ. Press, New York, 1999.

WASA Group, Changing waves and storms in the Northeast Atlantic? *Bull. Am. Meteorol. Soc.*, *79*, 741–760, 1998.

A. T. Cox, Oceanweather Inc., 5 River Road, Cos Cob, CT 06807. (andrewc@oceanweather.com)

V. R. Swail, Environment Canada, Toronto, Ontario, Canada M3H5T4.

(Received March 30, 2000; revised August 23, 2000; accepted August 31, 2000.)